Letters

Repairable, Recyclable, and Reliable Power Electronics Using Liquid Metal Interconnection

Wei Mu, *Member, IEEE*, Ameer Janabi, Zhongxiu Xiao, *Graduate Student Member, IEEE*, Chengjie Du, Luke Shillaber, and Teng Long, *Member, IEEE*

***Abstract*—The progression of power electronics technologies prioritizes efficiency and power density, often paying scant attention to the converter's own lifecycle environmental impact, resulting in significant and unnecessary waste. Traditional packaging and assembling methods of power electronic devices and converters rely on rigid bonding, such as soldering and sintering, to interconnect parts, causing challenges of disassembling and separating parts when repairing and recycling are needed. This letter introduces liquid metal (LM) as a bonding mechanism in power electronic device packaging and converter assembling. The fluidic interconnection using LM is invented to enable parts separation and thermomechanical stress reduction without compromising electrical performance. Therefore, repairable, recyclable, and reliable power electronics is achieved. Straightforward assembling and disassembling processes are demonstrated by a real repair case of the LM-based power stage. Electrical performance is validated by a buck converter, achieving an efficiency of up to 98.2%.**

***Index Terms*—Circular power electronics, lifecycle management thermomechanical stress, liquid metal (LM), reliability, repairable and recyclable converter.**

I. Introduction

DESIGN of power electronics has prioritized efficiency and power density, but often overlooks sustainability concerns [1]. However, as global energy systems shift toward electrification, the lifecycle environmental impact of power electronics equipment is becoming increasingly evident, particularly in terms of electronic waste generation [2]. More than five terawatts of equivalent power electronic hardware per year globally will be landfilled by 2050, causing significant material losses and environmental contamination [3].

Received 7 April 2025; revised 6 August 2025; accepted 29 August 2025. Date of publication 22 September 2025; date of current version 23 December 2025. This work was supported by the U.K. Research and Innovation (UKRI) Engineering and Physical Sciences Research Council (EPSRC) project Transforming Net Zero with Ultrawide Bandgap Semiconductor Device Technology (REWIRE) under Grant EP/Z531091/1. *(Corresponding author: Teng Long.)*

Wei Mu, Ameer Janabi, Zhongxiu Xiao, Chengjie Du, and Teng Long are with the Department of Engineering, University of Cambridge, Cambridge CB3 0FA, U.K. (e-mail: wm338@cam.ac.uk; ahaj2@cam.ac.uk; zx328@cam.ac.uk; cd900@cam.ac.uk; tl322@cam.ac.uk).

Luke Shillaber is with PMK IWATSU U.K. Ltd., Cambridgeshire PE16 6WA, U.K. (e-mail: luke.shillaber@pmk-iwatsu.co.uk).

Color versions of one or more figures in this article are available at https://doi.org/10.1109/TPEL.2025.3608127.

Digital Object Identifier 10.1109/TPEL.2025.3608127

Power electronic systems are composed of multiple functional and structural parts, such as semiconductors, passive components, current conductors, and cooling plates. These parts are interconnected by rigid joints formed through soldering or sintering processes, making them difficult to separate once the system is assembled. This irreversible assembling process causes difficulties in reusing or repairing parts of power electronic systems, causing significant waste of residual values when failures occur [4]. Without an effective separation or disassembling process, the highly heterogeneous power electronic systems are also difficult to be recycled, causing loss of precious materials [5]. Beyond repairability and recyclability challenges, conventional rigid joints formed through soldering and sintering are prone to fatigue failures over time due to mismatches in thermal expansion coefficients between bonded materials. This reliability concern becomes increasingly critical during the transition to wide bandgap semiconductors with smaller die sizes and greater thermal expansion mismatches [6].

Recent research highlights the need for a paradigm shift toward circular power electronics, where design strategies prioritize repairability, recyclability, and reliability (3Rs) from the outset. As emphasized in [7], developing renewable energy systems with longer lifecycles and improved repairability is critical for reducing environmental impact. Similarly, recyclability of powertrain components is essential to minimize material waste and enhance sustainability in electrified transportation [8]. A promising approach to achieving these goals is modular design, which facilitates disassembly, repair, and material recovery [9]. To support these efforts, life cycle assessment (LCA) frameworks have been developed to evaluate the environmental impact of power devices and guide more sustainable design decisions [10].

However, previous studies primarily emphasized the importance of circular design, proposed conceptual frameworks, or incorporated LCA considerations during the design phase. Technical solutions and engineering implementation to enable circular power electronics have been seldomly mentioned. One notable work [11] used a substrate-less power module, which eliminated nonrecyclable thermoset encapsulants and ceramic substrates. While the study provided a conceptual recycling process, the recyclability aspect has to be experimentally demonstrated. In addition, the separation process in [11] still requires

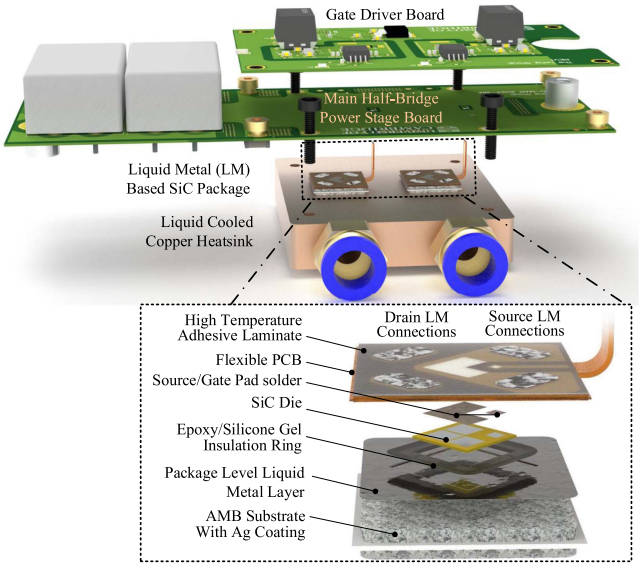

Fig. 1. Exploded view of the LM-based half-bridge power stage with detailed structure of LM-based embedded SiC package.

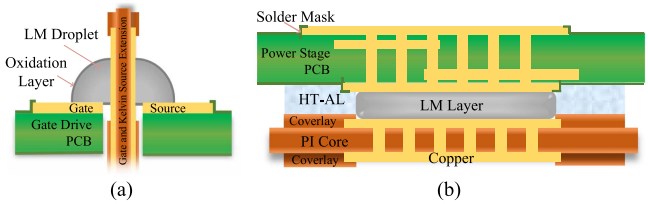

Fig. 2. Schematic of system-level LM interconnections: (a) gate/Kelvin-source signal interconnections and (b) drain/source power interconnections.

high-temperature treatments and chemical dissolution, which compromises its sustainability.

This study introduces an innovative interconnection approach that enables easy, room-temperature assembly and disassembly of components in power electronic systems, utilizing liquid metal (LM) as joints at both the semiconductor packaging [12] and system levels. The selected GaInAg LM alloy has high thermal and electrical conductivity but in liquid form at room temperatures. A new and exemplary half-bridge power stage assembly, as shown in Fig. 1, is proposed using SiC power MOSFETs to facilitate the implementation of LM joints. The assembling and disassembling processes of this power stage are elaborated to demonstrate the repairability and reusability of critical parts. In addition, this LM-based assembly effectively mitigates thermomechanical stress and warpage of the printed circuit board (PCB), which is commonly used as the power electronic system platform.

The rest of this letter is organized as follows. Section II introduces the power stage design and assembling process. Section III presents a real repair case and stress analysis, demonstrating 3Rs power electronics enabled by this new design. Section IV validates the performance of this power stage assembly used in a buck converter. Finally, Section V concludes this letter.

II. Converter Design and Assembling

Fig. 1 presents an exploded view of the modular half-bridge power stage assembly design for 3Rs considerations. The gate driver circuit is at the top. Just below it is the main half-bridge power stage board with dc-link and decoupling capacitors. The SiC device package is sandwiched between the main power PCB and a liquid-cooled copper heatsink. The exploded view at the bottom of Fig. 1 provides a detailed structure of the LM-based SiC package, which features a GaInAg LM fluidic connection and embedded floating die structure. This flexible PCB (FPCB)/die/AMB hybrid design combined with package-level LM connection can effectively reduce thermomechanical stress while maintaining high thermal and electrical conductivity required by the SiC device. The package-level detailed parameters, design considerations, and performance comparisons against state-of-the-art commercial packages are provided in [12] and [13], whereas this letter focuses on system-level integration and the demonstration of 3Rs. Screws on the power stage board are tightened using a torque screwdriver set to 0.1 N·m to ensure even and appropriate pressure, securing the package against the heatsink and enhancing thermal contact. This exerted force is sufficient to ensure optimal electrical and thermal connection via LM while also being beneficial for the package's structural integrity.

Both the signal connection and power connection are achieved by LM joints, as illustrated in Fig. 2. The FPCB of the LM-based package features a gate and Kelvin source extension, which can be easily bent upward and routed through the designated openings in both the power stage and gate drive PCB. Two LM droplets are deployed to establish electrical connections for the gate and Kelvin source. The schematic of this connection is shown in Fig. 2(a). Due to the high surface tension of LM ($\gamma >$ 500 mN/m), a droplet naturally forms at the corner between the FPCB gate/Kelvin source extension and the gate drive PCB. When exposed to ambient, the gallium in the GaInAg LM undergoes surface oxidation, forming a dense oxide layer just 0.7–3 nm thick. This oxidation layer acts as a shell [14], helping to maintain the shape and stability of the droplet [15]. Notably, the oxidation process is self-limiting due to the Cabrera–Mott mechanism, preventing further oxidation of the LM interior [16]. As a result, thermal and electrical conduction of the joint remains unchanged. The combined effects of high surface tension and the protective oxide layer ensure that the gate/Kelvin source connection remains well contained and does not spread or flow uncontrollably.

The top side of the FPCB is a layer of high-temperature nonwoven-carrier dual-sided tackified-acrylic adhesive laminate (HT-AL) with a thickness of 100 μm, as shown in Fig. 1, which is selectively removed over the copper pads through a die-cutting process. The HT-AL is intentionally not made too thin, as its nonwoven carrier provides both out-of-plane compressibility and in-plane shear compliance, enhancing the mechanical reliability of the interconnection. In addition, it helps accommodate excess LM and absorb manufacturing tolerances during assembly. A layer of LM with about the same thickness as the HT-AL is then applied to fill the cavity, forming the electrical connection between the power electronic device package and the

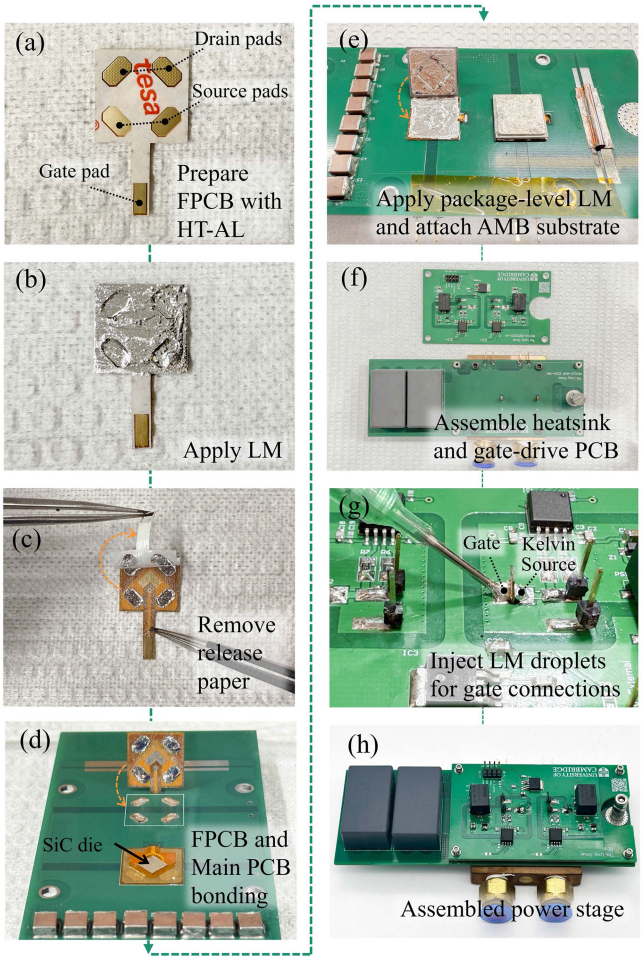

Fig. 3. Step-by-step assembly process of the LM-based power stage, conducted at room temperature and under the ambient atmosphere.

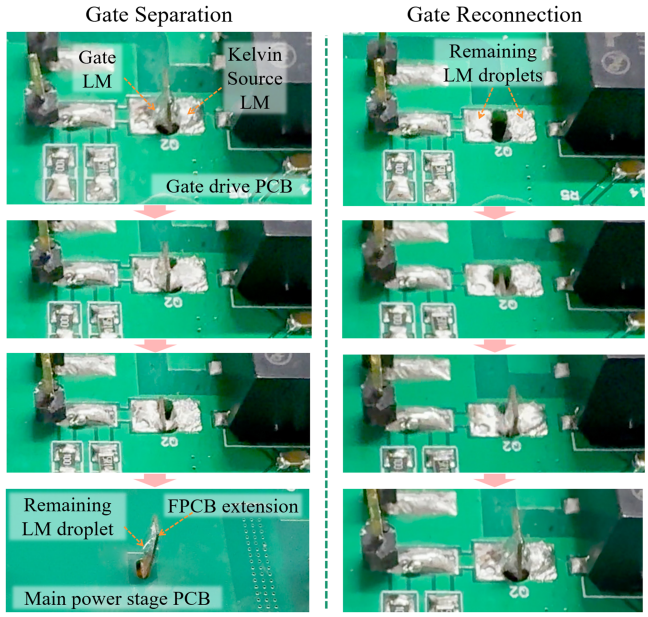

Fig. 4. Process of straightforward gate/Kelvin source LM contact separation and automatic reconnection.

system rigid PCB. As shown in Fig. 2(b), the FPCB is attached to the power stage rigid PCB using HT-AL, ensuring proper alignment of the solder pads on both the FPCB and PCB, which are connected via an LM layer. Notably, the combination of the coverlay and HT-AL effectively seals and contains LM.

The assembling process of the LM-based power stage is shown in Fig. 3(a)–(h). The bottom side of FPCB in (a) is premounted with the SiC MOSFET chip and surrounded by an insulation ring. The top side is laminated with precut HT-AL, which is covered by a silicone-coated release paper. LM is then applied to the top surface, and the amount of LM utilized is controlled using a syringe with a 21 G needle (0.60 mm inner diameter), which dispenses a ∼0.01 mL droplet. In this step, the release paper serves as a stencil, covering the HT-AL while exposing only the copper pads where electrical connections are required. As shown in Fig. 3(c), when the release paper is peeled off, the LM remains precisely on the pads defined by the HT-AL stencil. The strong surface tension of the LM, along with the thin oxide layer naturally formed on its surface, prevents spilling and keeps the LM confined within the designated cavities. This contracting force is strong enough to overcome gravity, as demonstrated in Fig. 3(d), where no dripping or displacement of LM is observed even when the FPCB is held vertically. This nanometer-thick oxide shell breaks upon touching the FPCB to the main power stage PCB, as a small force (0.5–0.6 N) can break this thin oxidation layer [17]. Therefore, the electrical and thermal contact between the LM and the interfacing surfaces remains largely unaffected by oxidation. After the AMB substrate wetted with LM is attached to the die-contact side of the FPCB (the bottom side of the FPCB) in Fig. 3(e), the copper heatsink is assembled to the backside, followed by the gate drive PCB on the top. LM droplets are then injected for the gate and Kelvin source connections, with contact pads acid-cleaned to improve wettability. It is worth noting that the entire assembly process is carried out at room temperature and under ambient atmospheric conditions, requiring minimal energy input and contributing to overall sustainability.

III. Demonstration of 3Rs in Power Electronics

A. Repairability and Recyclability

The power stage is designed so that the power electronics device chip of the power stage can be separated from the system PCB and heatsink when necessary without compromising performance. The gate drive PCB can be easily detached from the device and power stage PCB because the connection is made by LM droplets. As shown in Fig. 4, at the moment of removing the gate driver board, the withdrawing force simultaneously separates the LM droplet to disconnect the gate and Kelvin source connection. Remaining amounts of LM only stick on each copper pad, which has been originally wetted; thus, the through hole of the gate-source connection is clearly opened and ready to be retrofitted with a new or repaired device. When reinserting the FPCB extension into the designated openings, the connection is automatically restored. This process is realized

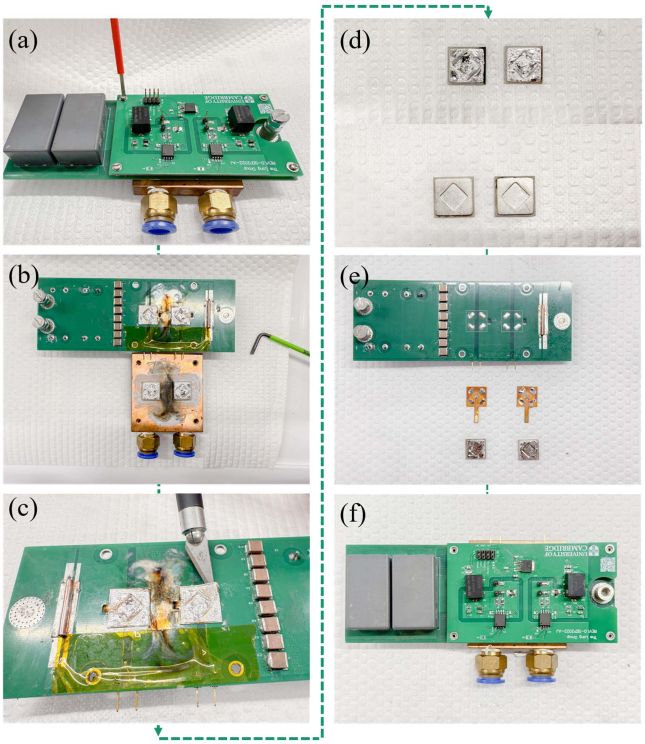

Fig. 5. Demonstration of the repairability of the LM-based power stage by replacing the failed SiC MOSFET while keeping the healthy parts intact: (a) separation of the gate-drive PCB, (b) separation of the LM package showing the failed device, (c) removal of the FPCB together with the failed device, (d) cleaning of the AMB substrate, (e) preparation of a new FPCB premounted with a SiC device and reapplication of LM, and (f) reassembly of the LM module.

by the unique microstructure and mechanical property of LM. The oxide layer enables the droplets to remain stable on the wetted surfaces during separation, while the high surface tension of LM allows the split droplets to recombine seamlessly upon recontact to minimize surface energy. This easily separable and reconnectable gate drive design and process greatly enhances the repairability of the power stage after commissioning and accelerates debugging and prototyping during development.

As shown in Fig. 5(a), a damaged module with both devices failed is identified. After disassembling the gate drive PCB and heatsink, the failure becomes clearly visible, as seen in Fig. 5(b). The FPCB, along with the failed devices, is removed by peeling off the HT-AL. The AMB substrate, PCB, and heatsink are then cleaned, and two new FPCBs with premounted SiC devices are prepared, as shown in Fig. 5(d) and (e). The power stage is reassembled following the same process described earlier in Fig. 3, and the integrated half-bridge is fully restored. Notably, the entire repair process is carried out at room temperature, requiring no additional energy input. The only materials used are a lint-free wipe and a small amount of isopropyl alcohol for cleaning, 1 g of the GaInAg LM (cost $\sim$ \$1), and the entire repair can be completed in 10 min.

The repairability of the LM-based power stage is further supported by analyzing changes in thermal and electrical conductivity before and after LM joint separation and reconnection. For the package-level LM layer, the volume fraction of oxide introduced during separation is given by:

$$\phi = \frac{V_{\text{ox}}}{V_{\text{LM}}} = \frac{2At_{\text{ox}}}{At_{\text{LM}}} = \frac{2t_{\text{ox}}}{t_{\text{LM}}}. \tag{1}$$

Here, A is the interfacial area, and the numerator is multiplied by 2 because both sides form oxide layers upon separation. At the package level, the LM thickness $t_{\text{LM}} = 30\ \mu$m, the oxidation layer thickness $t_{\text{ox}} = 3$ nm (worst case), and the resulting oxide volume fraction is 0.02%. To estimate the impact, the dilute-limit Maxwell–Garnett effective-medium framework can be utilized [18]. For any property P governed by the Laplace equation (including thermal conductivity k or electrical conductivity σ)

$$\frac{P_{\text{eff}}}{P_m} = \frac{P_i + 2P_m + 2\phi(P_i - P_m)}{P_i + 2P_m - \phi(P_i - P_m)} \tag{2}$$

where P_m is the property of the continuous matrix, P_i is the property of the inclusion phase, ϕ is the volume fraction of inclusions, and P_{eff} is the effective property of the composite. For the LM interconnections, Ga_2O_3 debris generated at each separation can be treated as an electrically and thermally insulating inclusion ($P_{\text{i}} \approx 0$) dispersed in the conductive LM matrix during subsequent reconnections. Therefore, (2) can be simplified as

$$\frac{P_{\text{eff}}}{P_m} = \frac{2P_m - 2\phi P_m}{2P_m + \phi P_m} = \frac{2(1-\phi)}{2+\phi}. \tag{3}$$

In previous analysis, $\phi \ll 1$, allowing (3) to be approximated by a first-order Taylor expansion as

$$\frac{P_{\text{eff}}}{P_m} = f(\phi) \approx 1 - \frac{3}{2}\phi + \mathcal{O}(\phi^2). \tag{4}$$

This corresponds to a relative performance degradation of $\Delta P/P_{\text{m}} = 0.03\%$ in both k and σ per separation–reconnection cycle. It noteworthy that, on the one hand, the dispersion of Ga_2O_3 fragments is uncertain and may be clustered or anisotropic, which can bias first-order effective-medium estimates upward. On the other hand, because the oxide formed per cycle is typically $<$3 nm, the actual degradation is expected to be smaller. Even so, under a conservative assumption of linear accumulation, approximately 33 cycles would be required for the cumulative change to reach 1%.

At the end of the power stage's service life, it can be either refurbished for reuse or disassembled for recycling. All components, including the gate drive PCB, power stage PCB, AMB substrate, and heatsink, can be easily separated without damage. The mechanical integrity of the PCB, power electronic die, and substrate remains intact, allowing for cleaning and reapplication of LM for continued use. If refurbishment is not feasible, the components can be individually sorted and recycled through appropriate processes. The ceramic substrate and heatsink can be recovered and reused, while the LM can be deoxidized, recycled, and reused [17]. This design supports both sustainability and circular economy principles in power electronics.

B. Reliability

Thermomechanical coupled finite element analysis is employed to evaluate the reliability advantages of utilizing LM interconnection on a half-bridge power stage. For a meaningful

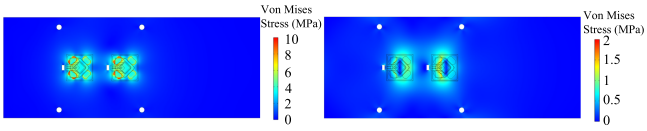

Fig. 6. Thermomechanical stress comparison of main power stage PCB using conventional soldered package (left) and proposed LM-based design (right).

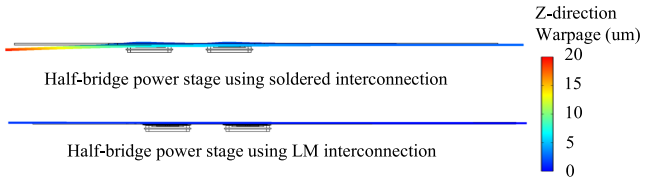

Fig. 7. Main power stage PCB Warpage (z-direction) comparison.

comparison, a conventional soldered counterpart is used as a baseline, in which both package-level and system-level interconnections are formed by solder. Apart from the interconnection method, all other design parameters are kept identical to ensure consistency in the comparison.

While the package-level thermal stress and reliability have been analyzed and validated in our previous study [12], simulation in this work focuses on the system-level reliability, specifically the thermal stress between the SiC package and the main power stage rigid PCB. The bottom surface of the AMB is modeled with a heat transfer coefficient of 6500 W/(m^2·K) and constrained using roller boundary conditions, representing the thermal dissipation and mechanical support provided by the heatsink. As shown in Fig. 6, under a uniform 100 W power dissipation per device, the LM-based power stage exhibits significantly lower thermal stress than the conventional soldered counterpart. This reduction is mainly due to the compliant nature of the LM layer, which effectively decouples thermal strain from the AMB substrate and prevents it from transferring to the PCB. This decoupling effect greatly enhances the reliability of the power stage by reducing the risk of thermal fatigue and material delamination, common failure mechanisms in power electronics.

An additional and direct benefit of using LM connections in the half-bridge assembly is the significant reduction in warpage, as shown in Fig. 7. Due to thermal expansion mismatch among different parts in power stage assembly, warpage occurs in conventional soldered designs, which degrades both electrical and thermal performance over time. The compliant LM layer effectively decouples this strain and almost eliminates warpage. This warpage reduction can directly improve the lifetime of the entire converter assembly [19].

Beyond thermal stress considerations, the mechanical reliability of LM joints under transient shocks was also evaluated. The gate/Kelvin source LM droplets rely on surface tension and a thin oxide layer for shaping, so the LM connections must not become a reliability constraint. Drop tests were conducted with the DUT placed horizontally and released onto a hard surface. To simulate mechanical shocks during rough handling, two drop severities were applied: 5 cm (typical) and 10 cm (harsher), in accordance with the IEC 60068-2-31 standard. As shown in Fig. 8, the LM droplets remained intact after the 5-cm drop and only shifted slightly downward after the 10-cm drop. This

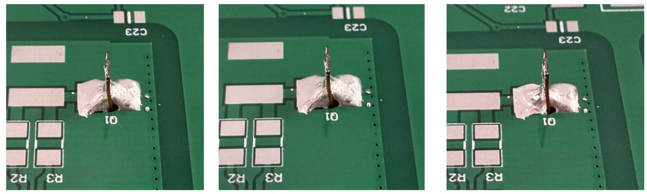

Fig. 8. LM-based gate/Kelvin source connections: (a) before the drop test, (b) after the 5-cm drop, and (c) after the 10-cm drop.

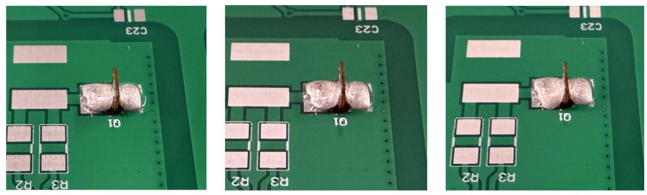

Fig. 9. LM-based gate/Kelvin source connections reinforced with silicone gel coating: (a) before, (b) after the 5-cm drop, and (c) after the 10-cm drop.

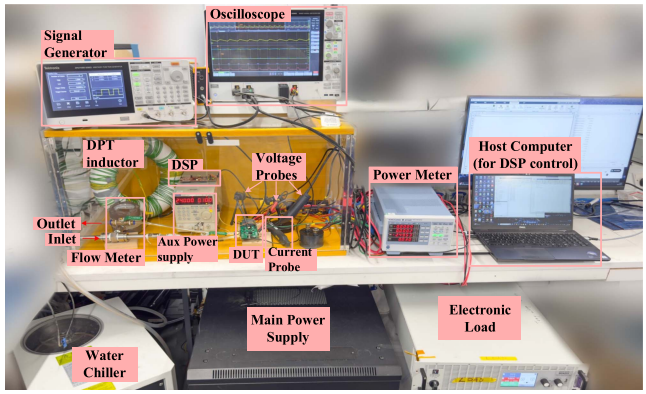

Fig. 10. Test setup for performance validation.

movement did not result in functional failure or risk of short circuit, as the droplets did not break apart due to the high surface tension of LM. Applying a thin silicone gel coating over the gate driver PCB effectively prevented any displacement (see Fig. 9). Furthermore, the power LM connections, including the package-level and system-level LM layers, are thin and externally sealed. They withstood a 1-m free-fall test without any sign of leakage, confirming the LM-based design's thermal and mechanical reliability.

IV. Performance Experiment Validation

Fig. 10 shows the experimental setup for performance evaluation. A synchronous buck converter was constructed to assess the performance of the LM-based power stage assembly in real power conversion applications. For comparison, an identical power stage with all interconnections achieved by soldering was tested. Because the power stage PCB has a low inductance design, zero-ohm gate resistors were used to achieve fast switching. The input voltage was set to 500 V, and various switching frequencies, duty cycles, and output currents were applied to evaluate performance under different operating conditions.

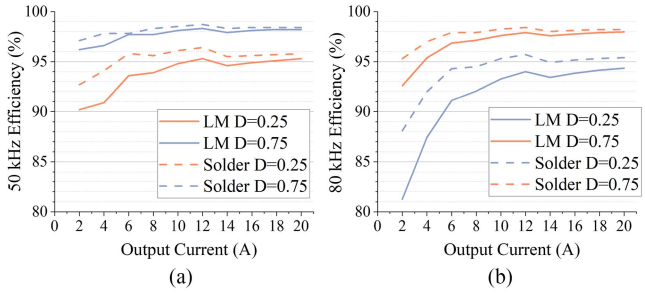

Fig. 11. Efficiency comparison of the synchronous buck converter operating under (a) 50 kHz and (b) 80 kHz.

Efficiency was measured by a power meter, and results are presented in Fig. 11. The LM-based converter exhibits slightly lower efficiency than the soldered counterpart under light load or high-frequency conditions. However, this difference diminishes as duty ratio or output current increases. The peak efficiency of the LM-based converter reaches 98.2% at 50 kHz and 98.0% at 80 kHz, less than 0.2% lower than the soldered counterpart.

V. Conclusion

This letter presents the potential of using LM in power electronics by introducing an LM-based power stage assembly that enables 3Rs. By replacing conventional solder joints with LM connections, the system achieves straightforward separation and reconnection of components, greatly simplifying and enabling repeated assembly and disassembly processes. High surface tension of LM, combined with its naturally formed dense oxide layer, reinforces the position of LM droplets at the correct connection points. The fluidic nature of LM joints at room temperature reduces thermomechanical stress. The inherently high thermal and electrical conductivity of LM ensures negligible compromise in performance. Together, this work provides a practical and scalable solution toward circular power electronics, aligning future converter design with the principles of environmental sustainability and lifecycle optimization.

References

[1] I. R. de Azua Lahidalga, E. M. Valor, D. J. Lozano, and J. M. F. Mendoza, "Circular power electronics: Exploring the scope and suitability of ecodesign criteria for the power electronics industry," in *Proc. Electron. Goes Green*, 2024, pp. 1–8, doi: 10.23919/EGG62010.2024.10631184.

[2] A. Sangwongwanich, D.-I. Stroe, C. Mi, and F. Blaabjerg, "Sustainability of power electronics and batteries: A circular economy approach," *IEEE Power Electron. Mag.*, vol. 11, no. 1, pp. 39–46, Mar. 2024, doi: 10.1109/MPEL.2024.3356248.

[3] J. Huber, L. Imperiali, D. Menzi, F. Musil, and J. W. Kolar, "Energy efficiency is not enough!," *IEEE Power Electron. Mag.*, vol. 11, no. 1, pp. 18–31, Mar. 2024, doi: 10.1109/MPEL.2024.3354013.

[4] L. Fang, P. Lefranc, and M. Rio, "Barriers for eco-designing circular power electronics converters," *Procedia CIRP*, vol. 116, pp. 287–292, Jan. 2023, doi: 10.1016/j.procir.2023.02.049.

[5] L. Braunwarth, S. Amrhein, T. Schreck, and M. Kaloudis, "Ecological comparison of soldering and sintering as die-attach technologies in power electronics," *J. Cleaner Prod.*, vol. 102, pp. 408–417, 2015,.

[6] W. Mu et al., "Direct integration of optimized phase-change heat spreaders into SiC power module for thermal performance improvements under high heat flux," *IEEE Trans. Power Electron.*, vol. 37, no. 5, pp. 5398–5410, May 2022, doi: 10.1109/TPEL.2021.3125329.

[7] G. Parise and M. Lombardi, "Ethics and eco-design for complex uses of energy: What we need for a sustainable future," *IEEE Ind. Appl. Mag.*, vol. 28, no. 5, pp. 74–79, Sep./Oct. 2022, doi: 10.1109/MIAS.2022.3160998.

[8] C. Antoniou et al., "Life cycle analysis of power electronics and electric machines for future electrified passenger cars," in *Powertrain Systems for Net-Zero Transport*. Boca Raton, FL, USA: CRC Press, 2021, pp. 315–332.

[9] T. T. Romano, T. Alix, Y. Lembeye, N. Perry, and J. C. Crébier, "Towards circular power electronics in the perspective of modularity," *Procedia CIRP*, vol. 116, pp. 588–593, 2023.

[10] P. Stanchev, G. Vacheva, and N. Hinov, "Review of methodologies for life cycle assessment of power electronic devices," in *Proc. 7th Junior Conf. Lighting*, 2022, pp. 1–4, doi: 10.1109/Lighting56379.2022.9929154.

[11] J. Wei et al., "Substrate-less power semiconductor packaging for the potential of recyclability," *IEEE J. Emerg. Sel. Top. Power Electron.*, vol. 13, no. 2, pp. 2158–2172, Apr. 2025, doi: 10.1109/JESTPE.2025.3540294.

[12] W. Mu, A. Janabi, B. Hu, L. Shillaber, and T. Long, "Liquid metal fluidic connection and floating die structure for ultralow thermomechanical stress of SiC power electronics packaging," *IEEE Trans. Power Electron.*, vol. 39, no. 7, pp. 7808–7814, Jul. 2024, doi: 10.1109/TPEL.2024.337912.

[13] A. Janabi et al., "Substrate embedded power electronics packaging for silicon carbide MOSFETs," *IEEE Trans. Power Electron.*, vol. 39, no. 8, pp. 9614–9628, Aug. 2024, doi: 10.1109/TPEL.2024.3396779.

[14] S. Amini et al., "Interplay between interfacial energy, contact mechanics, and capillary forces in EGaIn droplets," *ACS Appl. Mater. Interfaces*, vol. 14, no. 24, pp. 28074–28084, 2022.

[15] Y. Ding, M. Zeng, and L. Fu, "Surface chemistry of gallium-based liquid metals," *Matter*, vol. 3, no. 5, pp. 1477–1506, 2020.

[16] W. Babatain, M. S. Kim, and M. M. Hussain, "From droplets to devices: Recent advances in liquid metal droplet enabled electronics," *Adv. Function Mater.*, vol. 34, no. 31, 2024, Art. no. 2308116.

[17] M. D. Dickey, "Emerging applications of liquid metals featuring surface oxides," *ACS Appl. Mater. Interfaces*, vol. 6, no. 21, pp. 18369–18379, 2014.

[18] K. B. Kiradjiev, S. A. Halvorsen, R. A. Van Gorder, and S. D. Howison, "Maxwell-type models for the effective thermal conductivity of a porous material with radiative transfer in the voids," *Int. J. Thermal. Sci.*, vol. 145, 2019, Art. no. 106009.

[19] Y. Guo, "Reliability sensibility analysis of the PCB assembly concerning warpage during the reflow soldering process," *Mathematics*, vol. 10, 2022, Art. no. 3055, doi: 10.3390/math10173055.